Kinetics and Catalysis, Vol. 42, No. 4, 2001, pp. 574–581. Translated from Kinetika i Kataliz, Vol. 42, No. 4, 2001, pp. 632–640.
Original Russian Text Copyright © 2001 by Bychkov, Sinev, Vislovskii.

Thermochemistry and Reactivity of Lattice Oxygen in V–Sb Oxide Catalysts for the Oxidative Dehydrogenation of Light Paraffins

V. Yu. Bychkov*, M. Yu. Sinev*, and V. P. Vislovskii**
** Semenov Institute of Chemical Physics, Russian Academy of Sciences, Moscow, 117977 Russia*
*** Azerbaijan Institute of Inorganic and Physical Chemistry, Academy of Sciences of Azerbaijan, Baku, Azerbaijan*

Received May 29, 2000

Abstract—Differential scanning calorimetry is used to study *in situ* the properties of strongly bound (lattice) oxygen in vanadium-containing supported catalysts for the oxidative dehydrogenation of paraffins C_2–C_4. Evidence is found that the process occurs via a stepwise redox mechanism with the participation of lattice oxygen from the catalyst. When the supported component is modified by an antimony additive, the amount of reactive oxygen increases and redox processes accelerate. Simultaneously, the rate of coke formation decreases. Additional modification by Bi and Ba leads to a further increase in the amount of reactive oxygen. In all cases, oxygen bound to vanadium atoms is responsible for the redox properties of the systems. The observed effects are analyzed from the standpoint of the ratio between different forms of active oxygen.

INTRODUCTION

Oxidative dehydrogenation of light paraffins is given attention as a potential process for the synthesis of valuable alkenes, for which demand is constantly growing. The absence of efficient catalysts that would combine high productivity, selectivity to olefins, and stability prohibit this process from being widely used in industrial practice. Currently, this problem remains unsolved despite intensive studies along these lines (see, for instance, review papers [1–3]).

Of all catalysts, vanadium-containing systems, which are efficient in the oxidative dehydrogenation of paraffins C_2–C_4 at temperatures above 500°C, attract the greatest attention. However, these systems have some limitations: they rapidly lose activity during the catalytic process and their selectivity is not high in some cases.

Earlier, when studying the oxidative dehydrogenation of propane and isobutane, we showed [4] that vanadium-containing oxide systems supported on Al_2O_3 are more active and selective than bulk catalysts and that their catalytic properties are substantially improved when the composition of the supported component becomes somewhat more complex. Literature data on the structures of supported vanadium-containing systems and on the mechanism of their catalytic action usually refer to nonmodified samples (see, for instance, review papers [5, 6]). Therefore, it is interesting to determine which of the properties of a supported system change upon modification and trace how these changes are reflected in the catalytic properties.

Note that the widely used kinetic model of catalytic processes that occur via the stepwise redox mechanism was first developed by Mars and van Krevelen to describe the oxidation of aromatic hydrocarbons on a supported vanadium-containing (V–Mo–P/Al_2O_3) catalyst [7]. Since that time, many catalytic oxidation reactions were found to occur via the redox mechanism. In the simplest case, the process is described by the scheme

$$LO + A \longrightarrow L + AO, \qquad (Ia)$$

$$L + 1/2O_2 \longrightarrow LO. \qquad (Ib)$$

In step (Ia), the oxidative site LO on the surface is reduced by the reactant molecule A to form the oxidation product AO. In step (Ib), the reduced site L is oxidized by oxygen from the gas phase. It is important that oxygen capable of transferring to the product is so strongly bound to the catalyst that step (Ib) can be considered irreversible. Due to the high binding strength, oxygen is often considered to belong to the oxide lattice (which explains the term *lattice oxygen*).

Mars and van Krevelen [7] derived and analyzed the rate law named after them:

$$w = \frac{k_{red}k_{ox}[A]^m[O_2]^n}{k_{red}[A]^m + k_{ox}[O_2]^n}, \qquad (1)$$

where w is the rate of the steady-state process; k_{red} and k_{ox} are the rate constants of steps (Ia) and (Ib), respectively; [A] and $[O_2]$ are the concentrations of reactants in the gas phase; m and n are the kinetic orders of steps (Ia) and (Ib) with respect to reactants A and O_2, respectively.

Since step (Ib) is virtually irreversible, Eq. (1) does not include adsorption/desorption terms. A guideline in deciding whether the process belongs to this class is the equality or proximity of the rates of product formation at the steady state and in the absence of oxygen in the gas phase when the degree of catalyst oxidation is close to a stationary one. This makes it possible to study the regularities of the steps of catalyst reduction with product formation (Ia) and reoxidation (Ib) separately.

According to the published data [5, 6], even nonmodified supported vanadium catalysts contain different forms of the active component (monomeric and polymeric surface structures containing vanadium ions with different coordination, clusters, and crystallites of vanadium oxides having different sizes, structures, and morphology). These forms are present in different concentrations in the samples depending on the type of support, the concentration of active component, and the preparation procedure. They have different reactivities and contribute differently to the overall reactivity of the system and to the overall catalytic process.

It follows from reactions (Ia) and (Ib) and Eq. (1) that the whole set of contributes properties of the catalytic system is reflected in the reaction through the reactivity of active oxygen forms. Thus, the characteristics of oxygen largely determine the overall activity and selectivity of the catalyst. One of the main characteristics is the binding energy of oxygen with the oxide lattice, because this value contributes the activation energies of both steps ((Ia) and (Ib)) and, therefore, determines the overall process rate [8]. As noted above, the oxide system contains several structures, which tend to change during the process. Consequently, the properties of reactive oxygen are nonuniform from the beginning and also change in redox transformations.

In view of the above information, our goal was to trace how the complication of the elemental composition of supported catalysts changes the thermochemical parameters and reactivity in the processes of oxygen exchange with gas-phase molecules. Our method was based on finding the relationships between the extent of reduction, oxygen binding energy, reactivity, and selectivity. Differential scanning calorimetry (DSC) was used *in situ* together with pulsed supply of reactants. This enabled us to trace the dynamics of the state of the catalyst active component, which directly participates in the reaction in the catalytic system [9].

The methods for estimating the strength of oxygen binding to the catalyst can be categorized as direct and indirect. Indirect methods are temperature-programmed desorption (TPD) of oxygen and temperature-programmed reduction (TPR). The direct determination of thermal effects in reactions with scission and formation of oxygen bonds with a lattice (catalyst reduction and reoxidation) can be done using calorimetric measurements. TPD/TPR methods make it possible to separate the desorption processes of different oxygen forms over temperatures. However, they usually do not distinguish the effects of energy and other factors that determine temperature intervals of registered processes. Also, the TPD method is better applicable to weakly bound forms of oxygen. Calorimetry is a universal method, but it has limited sensitivity and somewhat low temporary resolution. Therefore, it is more suitable for more firmly bound oxygen compared to TPD. The *in situ* DSC method makes it possible to combine advantages of both approaches and characterize the complete spectrum of oxygen forms.

Vanadium-containing samples supported on γ-Al_2O_3 were chosen for the study. These samples differed in the concentrations of modifying additives. The study of catalytic properties of these samples in the oxidative dehydrogenation of C_2–C_4 paraffins has been carried out earlier [4]. Because the use of calorimetric data for calculating the strength of oxygen binding to the lattice requires some quantitative information on the formation of all products of paraffin oxidation (carbon oxides, olefins, partial oxidation products, cracking products, etc.), more errors may appear in quantitative measurements when the initial molecule becomes more complex. Therefore, in this work, we used ethane as a model substance. In some cases, hydrogen is used as a reducing agent.

In this work, we do not discuss the details of the phase composition and structure of the surface of our samples. These issues are considered elsewhere [4].

EXPERIMENTAL

We studied samples with the following compositions: 5.83% V_2O_5/γ-Al_2O_3, 11.9% Sb_2O_3/γ-Al_2O_3, 5.83% V_2O_5–11.9% Sb_2O_3/γ-Al_2O_3, and 5.5% V_2O_5–11.5% Sb_2O_3–5.5% Bi_2O_3–0.1% BaO/γ-Al_2O_3. These are denoted henceforth as follows: V/Al_2O_3, Sb/Al_2O_3, V–Sb/Al_2O_3, and V–Sb–Bi–Ba/Al_2O_3, respectively. The samples were prepared by the impregnation of support (microspherical γ-Al_2O_3 supplied by MNTK Katalizator, Novosibirsk; the specific surface area was 85 m^2/g; the particle size was 0.3–0.8 mm) by aqueous solutions of ammonium metavanadate, $SbCl_3$, and bismuth and barium nitrates taken in appropriate amounts.

The interaction with reducing gases (hydrogen, ethane, and ethane–helium mixtures) and air was studied in a setup that involved a DSC-111 scanning calorimeter and two gas chromatographs. A sample loading (80–100 mg) was charged into a quartz cell, which was then placed into a measurement channel of the calorimetric block of the calorimeter. Preliminary treatment of the samples included heating in a flow of air at 650°C for 30 min and cooling to 550°C in a flow of air. During a run, samples were purged by specially purified helium at a flow rate of 30 ml/min. Pulses of reaction gases (0.5 ml each) were dosed into a helium flow using a six-way valve. The flow passed over a sample and then to two serial chromatographs for analyses. Columns were packed with Porapak N and zeolite 5A. Thermal-conductivity detectors were used. The system allowed us to measure the concentrations C_2H_6, C_2H_4, CO_2, H_2, O_2, N_2, CH_4, and CO.

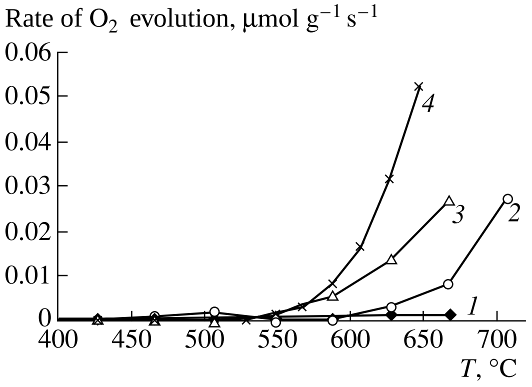

Fig. 1. TPD of oxygen from the samples (*1*) V/Al_2O_3, (*2*) Sb/Al_2O_3, (*3*) $V–Sb/Al_2O_3$, and (*4*) $V–Sb–Bi–Ba/Al_2O_3$.

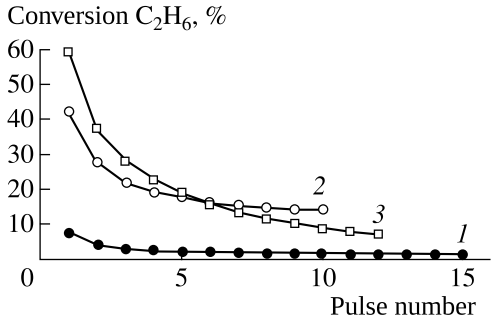

Fig. 2. Ethane conversion during the interaction of the samples with 35% ethane + He pulses at 550°C: (*1*) Sb/Al_2O_3, (*2*) V/Al_2O_3, and (*3*) $V–Sb/Al_2O_3$.

To strike a carbon balance more reliably, the selectivity to ethylene was calculated using two methods:

$$S_1 = 2C_{C_2H_4}/(C_{CO_2} + C_{CO} + 2C_{C_2H_4}) \times 100\%,$$

$$S_2 = C_{C_2H_4}/(C^0_{C_2H_6} - C_{C_2H_6}) \times 100\%,$$

where C_i is the volume concentration of ethane or the products of its conversion (vol %) and $C^0_{C_2H_6}$ is the volume concentration of ethane when no reaction occurs (vol %).

At all temperatures, water is evolved in the interaction of the systems with ethane or hydrogen immediately after passing a reducing-gas pulse. Therefore, a calorimetric signal consisted of a narrow exothermic part and a broad endothermic part [9]. Their algebraic sum is the overall thermal effect of the reaction between hydrogen (Q_{H_2}) and ethane ($Q_{C_2H_6}$):

$$H_2 + |O|_L \longrightarrow H_2O + |\,|_L, \quad +Q_{H_2}, \text{ kJ/mol } H_2$$

$$C_2H_6 \xrightarrow{|O|_L} xC_2H_4 + yCO$$

$$+ zCO_2 + (6 - 4x)/2H_2O, \quad +Q_{C_2H_6}, \text{ kJ},$$

where $|O|_L$ and $|\,|_L$ are the lattice oxygen atom and an oxygen vacancy, respectively. Since the reaction with ethane yields many products, the value of $Q_{C_2H_6}$ was not referred to any specific substance.

The values of Q_{H_2} and $Q_{C_2H_6}$ can be used as a basis to calculate the thermochemical characteristics of catalyst oxygen that reacted with the pulse of reducing agent pulse. This can be done if we take into account the heats of overall reactions

$$2H_2 + O_2 \longrightarrow 2H_2O, \quad Q_1 = 241.8 \text{ kJ/mol } H_2,$$

$$C_2H_6 + 7/2O_2 \longrightarrow 2CO_2 + 3H_2O,$$

$$Q_2 = 713.8 \text{ kJ/mol } CO_2,$$

$$C_2H_6 + 5/2O_2 \longrightarrow 2CO + 3H_2O,$$

$$Q_3 = 430.8 \text{ kJ/mol CO},$$

$$C_2H_6 + 1/2O_2 \longrightarrow C_2H_4 + H_2O,$$

$$Q_4 = 104.8 \text{ kJ/mol } C_2H_4.$$

The thermochemistry of lattice oxygen can be characterized quantitatively using different values related to each other by simple linear relationships. These are, for instance, the heat of MO_x oxide formation or the binding energy of oxygen to the lattice. For convenience, we chose the heat of reoxidation (Q_{ox}) of the reduced oxide:

$$O_2 + 2|\,|_L \longrightarrow 2|O|_L, \quad +Q_{ox}, \text{ kJ/mol } O_2.$$

The value of Q_{ox} is measured directly in the calorimetric experiment on the reoxidation of a sample containing oxygen vacancies $|\,|_L$. It can also be calculated from experimentally measured heat of sample reduction by hydrogen (Q_{H_2}) or ethane ($Q_{C_2H_6}$) using the following formulas

$$Q_{ox} = 2Q_1 - 2Q_{H_2},$$

$$Q_{ox} = (n_{CO_2}Q_2 + n_{CO}Q_3 + n_{C_2H_4}Q_4 - Q_{C_2H_6})/n_{O_2}.$$

where n_i is the number of moles of the *i*th substance (a reacted reducing agent or a product), n_{O_2} is the number of moles of oxygen supplied by the oxide to form the necessary amount of oxidation products.

The accuracy of calorimetric measurements is about 1.0%, as it was determined by measuring the heats of standard sample melting (aluminium and zinc).

Temperature programmed desorption of oxygen was studied at temperatures ranging from 50 to 700°C and a heating rate of 10°C/min. Helium flow through a cell with a sample had a rate of ~5 ml/min from which samples were withdrawn for chromatographic analyses. In the case of vanadium-containing samples, temperature was kept below ~650°C to prevent V_2O_5 melting.

The detailed description of the setup with the DSC-111 calorimeter and chromatographic analysis of the gas phase, the system for gas supply, and purification of the carrier gas (helium) were described in [10].

RESULTS

Thermal Desorption of Oxygen

Thermal desorption data for oxygen are shown in Fig. 1. The overall amounts of oxygen evolved during thermal desorption and further keeping samples for 25–30 min at a final temperature after their heating are specified in Table 1. An insignificant amount of oxygen is evolved from the V/Al_2O_3 sample. Desorption from the Sb/Al_2O_3 sample becomes more pronounced starting from 590°C. However, in the case of $V–Sb/Al_2O_3$, the amount of desorbed oxygen is much larger even at 530°C.

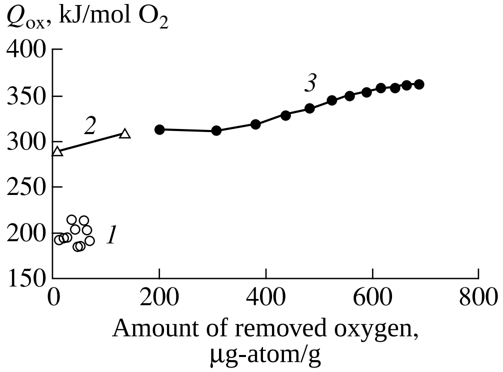

Fig. 3. Dependence of Q_{ox} on the amount of oxygen removed from the samples (*1*) Sb/Al_2O_3, (*2*) V/Al_2O_3, and (*3*) $V–Sb/Al_2O_3$.

Reduction of Samples

Sb/Al_2O_3. The interaction of the Sb/Al_2O_3 sample with pulses of the 10% H_2 + He mixtures was studied at 550°C. This is lower than temperature when thermal desorption of oxygen from Sb/Al_2O_3 begins. Therefore, before the beginning of reduction, oxygen removed by TPD is present in the sample. During reduction 68 µmol H_2/g was consumed and 34 µmol O_2/g was removed. Figure 2 shows the values of ethane conversions in the reaction of the Sb/Al_2O_3 sample with 35% ethane pulses at 550°C. Table 1 indicates the overall amounts of removed oxygen.

These data show that about the same amount of oxygen (~30 µmol/g) of the Sb/Al_2O_3 system can react with hydrogen or ethane and evolve during TPD.

During the interaction of Sb/Al_2O_3 with ethane, we observed a triple increase in the ratio of the evolved heat vs reacted ethane. This points to the occurrence of an additional thermal process whose nature is unclear. We failed to calculate Q_{ox} for this run. This value can be calculated from the runs on the reduction of the sample with hydrogen. The experimental data are summarized in Fig. 3.

The Sb/Al_2O_3 sample reduced by ethane at 550°C can be reoxidized to the initial state in a flow of air at 650°C with further cooling in a flow of air to 550°C. Second reduction is virtually identical to the first one in this case. However, the interaction of the sample reduced by ethane at 550°C with air pulses at 550°C does not lead to the noticeable consumption of oxygen and the corresponding heat evolution. The formation of carbon oxides was not observed either. That is, when ethane interacts with the sample at 550°C sample is not coked.

V-containing systems. Figures 2 and 4 show the data on ethane conversion and selectivity to ethylene when 35% ethane + He pulses interact with the V/Al_2O_3 sample. The conversion is several times higher than on Sb/Al_2O_3. As follows from Table 1, V/Al_2O_3 loses a considerable amount of oxygen in this process. Assuming that the initial state corresponds to the V_2O_5 stoichiometry, it changes during the experiment and becomes $V_2O_{4.14}$. Furthermore, in the process of ethane oxidation, the sample is substantially coked. This follows from the comparison of the selectivity values for ethylene S_1 and S_2: S_1 takes into account only gaseous products being much higher than S_2. For this run, carbon imbalance is 187 µmol C_2H_6/g. During the reoxidation of the reduced sample, we observed the evolution of CO_2 in large amounts.

Intensive coking prevented us from calculating the values of Q using the data of this experiment, but we managed to measure the strength of oxygen binding for the V/Al_2O_3 sample using hydrogen as a reducing agent. In the case of hydrogen, lower extents of vanadium reduction are observed. The resulting data are presented in Fig. 3.

Figures 2 and 4 show the experimental data for the interaction of the $V–Sb/Al_2O_3$ sample with helium pulses containing 35% ethane. It is seen that, in this case, the conversion of ethane and the amount of active oxygen are greater than for V/Al_2O_3: if we again consider that the initial state is V_2O_5, then it becomes V_2O_3

Table 1. Overall amount of oxygen removed during thermal desorption and during the interaction of the catalyst with 10–15 pulses of ethane

Sample	TPD, µmol O_2/g	Reduction, µmol O_2/g*
Sb/Al_2O_3	28.0	31.5
V/Al_2O_3	0.9	128.0
$V–Sb/Al_2O_3$	52.0	370.5
$V–Sb–Bi–Ba/Al_2O_3$	35.0	443.5

* Calculated as the overall amount of oxygen removed as O_2 and products of ethane oxidation.

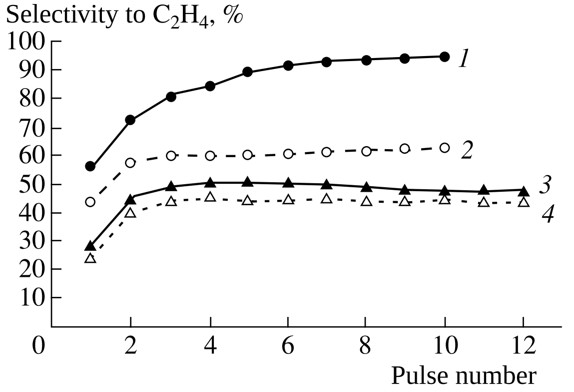

Fig. 4. Selectivity to ethylene in the reaction between the samples (*1*, *2*) V/Al_2O_3 and (*3*, *4*) $V–Sb/Al_2O_3$ and 35% ethane + He pulses at 550°C calculated from the overall amount of products (S_1, curves *1* and *3*) and ethane conversion (S_2, curves 2 and *4*).

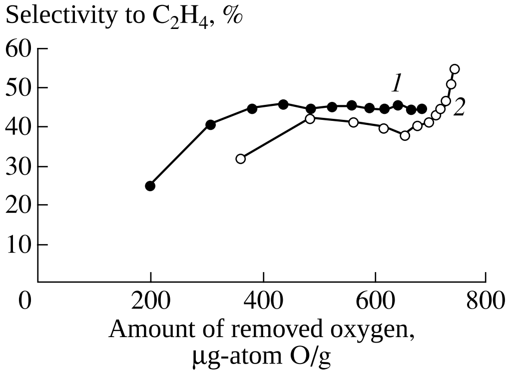

Fig. 5. Selectivity to ethylene S_1 vs. amount of oxygen removed from the $V–Sb/Al_2O_3$ sample in the reaction with (*1*) 35% ethane + He and (*2*) 100% ethane pulses at 550°C.

after the reaction. The selectivities to ethane S_1 and S_2 are close, which points to low coking. During reoxidation of the $V–Sb/Al_2O_3$ sample reduced by ethane, only 0.55 μmol CO_2/g evolved.

In contrast to the V/Al_2O_3 sample, at a low extent of reduction, the $V–Sb/Al_2O_3$ sample gives mostly carbon oxides. If before the beginning of reduction by ethane, the $V–Sb/Al_2O_3$ sample is heated in a flow of the inert gas at 550°C, the selectivity to ethylene in the first pulse increases by 7–8%. In further reduction of $V–Sb/Al_2O_3$, the selectivity increases, but remains lower than S_1 in the case of V/Al_2O_3. The selectivity does not increase monotonically, but has a slight maximum at an intermediate extent of reduction.

Figure 5 shows a change in the selectivity to ethylene depending on the amount of oxygen removed from the $V–Sb/Al_2O_3$ catalyst. The use of 100% ethane pulses results in deeper reduction of the $V–Sb/Al_2O_3$ system. At the same time, a drastic growth in the selectivity is observed when ~700 μg-at O/g is removed.

The reduction of $V–Sb/Al_2O_3$ by ethane is accompanied by an increase in the binding energy of oxygen being removed from the sample (see Fig. 3).

The reoxidation of vanadium-containing samples by oxygen pulses at 550°C is much faster than in the case of Sb/Al_2O_3. For the $V–Sb/Al_2O_3$ sample reduced by ethane, reoxidation by several pulses of air results in the complete recovery of the catalyst except for the least weakly bound oxygen, which shows itself in the first TPD pulse during reduction by ethane.

The $V–Sb–Bi–Ba/Al_2O_3$ sample contains more active oxygen than any other catalyst studied in this work (see Fig. 1 and Table 1). The reduction of $V–Sb–Bi–Ba/Al_2O_3$ was studied using pulses with different ethane concentrations: 12.3, 35.0, and 100%. Figure 6a shows the values of the selectivity to ethylene depending on the amount of oxygen removed from $V–Sb–Bi–Ba/Al_2O_3$ during reduction by ethane pulses. As in the case of $V–Sb/Al_2O_3$, the interaction of ethane with the completely oxidized sample mostly leads to the formation of carbon oxides. The selectivity increases with an increase in the extent of $V–Sb–Bi–Ba/Al_2O_3$ reduction and reaches the maximum (~50%) when 300–350 μg-atom/g of oxygen is removed. Further reduction leads to a decrease in the selectivity to ~40%.

The $V–Sb–Bi–Ba/Al_2O_3$ sample was not cocked in reduction by ethane, so we were able to calculate Q_{ox}. Figure 6b shows the values of Q_{ox} depending on the extent of sample reduction achieved in the experiment.

Interaction with the Ethane–Air Mixture in a Pulse Mode

The interaction of samples with pulses of the ethane–air mixture allowed us to correlate a change in the catalytic activity and selectivity of the system with the extent of catalyst reduction. Figure 7 shows data on the ethane conversion, the selectivity to ethylene, and the amount of oxygen removed during the interaction of 15% ethane + 25% air + helium pulses with $V–Sb–Bi–Ba/Al_2O_3$ at 550°C. During the first pulses, the catalyst is partially reduced. Then, the reaction rates approach some constant (“stationary”) value. A similar behavior was observed for other samples as well. Table 2 shows the parameters of the catalytic reaction at this state and the amounts of oxygen removed during the experiment.

DISCUSSION

The results of this study point to a substantial difference in Sb/Al_2O_3 and vanadium-containing samples. Because approximately the same amount of oxygen (~30 μmol/g) in the Sb/Al_2O_3 sample can react with hydrogen or ethane and evolve in TPD, we conclude that only one form of active oxygen is present in the system. According to the reference data [11], the following consecutive oxidative transformations can occur in the antimony–oxygen system:

$$2Sb + 3/2O_2 \longrightarrow Sb_2O_3,\ -471.52\ \text{kJ/mol}\ O_2, \quad \text{(II)}$$

$$Sb_2O_3 + 1/2O_2 \longrightarrow Sb_2O_4,\ -383.04\ \text{kJ/mol}\ O_2, \quad \text{(III)}$$

$$Sb_2O_4 + 1/2O_2 \longrightarrow Sb_2O_5,\ -171.36\ \text{kJ/mol}\ O_2. \quad \text{(IV)}$$

The values of Q_{ox} found in our experiments for Sb/Al_2O_3 ~200 kJ/mol O_2) correspond only to the transition from Sb_2O_5 to Sb_2O_4. It is likely that some portion of antimony in Sb/Al_2O_3 is capable of being oxidized to Sb(V) as a result of treatment in anair flow at 650°C. Then, it is reduced by the reaction with hydrogen or ethane.

In the vanadium–oxygen system, many oxide phases are known, which are intermediate between V_2O_3 and V_2O_5 [12]. The heats of some consecutive oxygenation processes are shown below. These heats are calculated from the enthalpies of formation of individual oxides:

$$2VO + 1/2O_2 \longrightarrow V_2O_3,\ -710\ \text{kJ/mol}\ O_2, \quad \text{(V)}$$

$$V_2O_3 + 1/2O_2 \longrightarrow V_2O_4,\ -442\ \text{kJ/mol}\ O_2, \quad \text{(VI)}$$

$$V_2O_4 + 1/2O_2 \longrightarrow V_2O_5,\ -224\ \text{kJ/mol}\ O_2. \quad \text{(VII)}$$

Comparison of these values with data shown in Fig. 3 suggests that the heats expected for the transition between V^{3+} and V^{2+} are not observed in the experiment. It is likely that a gradual change in the Q_{ox} value points to almost continuous series of transitions between the states of vanadium ions from V^{5+} to V^{3+}, which are within the interval of the heats of reactions (VI) and (VII).

Our data on the heats of supported vanadium oxide oxidation agree well with earlier results [13] for the oxidation heats of hydrogen-reduced $V_2O_5/\gamma\text{-}Al_2O_3$ measured by an analogous DSC-111 calorimeter. Andersen and Kung [13] also observed a continuous change in the heat of vanadium oxide oxidation depending on the extent of reoxidation in the interval between 200 and 360 kJ/(mol O_2).

However, we failed to reproduce the results obtained by Bars *et al.* [14], who studied the reduction of $V_2O_5/\gamma\text{-}Al_2O_3$ by ethane and found the removal of up to 3.8 oxygen atoms per one vanadium atom during reduction at 450°C. In our experiments, the extent of reduction was at most 1–1.2 oxygen atoms per vanadium atom.

From the standpoint of understanding the mechanism of catalytic action, an important issue is the effect of vanadium component modification on its properties. Oxygen TPD data (Fig. 1 and Table 1) show that, in the case of the two-component $V–Sb/Al_2O_3$ system, the amount of desorbed oxygen substantially increases compared to one-component systems, and desorption begins at a lower temperature. This may indicate that a new form of active oxygen is present in the mixed system.

A relatively low selectivity to ethylene in the first pulses of the $V–Sb/Al_2O_3$ sample reduction by ethane and an increase in the selectivity after preliminary heating points to the fact that active oxygen that desorbs at 530–670°C during TPD is responsible for an increase in the rate of complete oxidation.

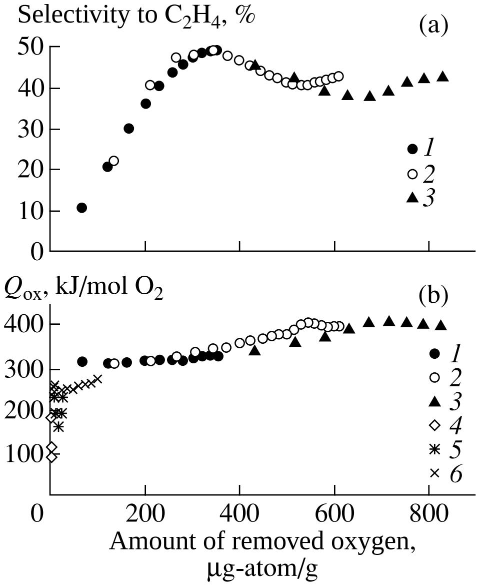

Fig. 6. Dependence of (a) the selectivity S_1 to ethylene and (b) Q_{ox} on the amount of oxygen removed during the interaction of $V–Sb–Bi–Ba/Al_2O_3$ with pulses of mixtures containing (*1*) 12.3, (*2*) 35, and (*3*) 100% ethane in helium at 550°C and 10% H_2 + He at 300°C at (*4*) 300, (*5*) 400, and (*6*) 550°C.

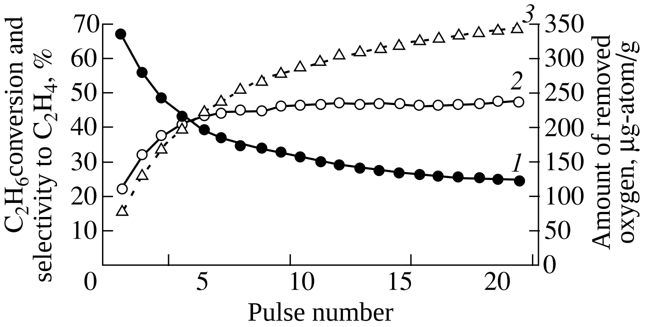

Fig. 7. Interaction of $V–Sb–Bi–Ba/Al_2O_3$ with pulses 15% C_2H_6 + 25% air + He at 550°C: (*1*) ethane conversion, (*2*) selectivity to ethylene, and (*3*) amount of oxygen removed from the catalyst.

The use of pure ethane pulses results in the deeper reduction of the $V–Sb/Al_2O_3$ system. At high extents of reduction, a drastic increase in the selectivity is observed. It is likely that the process mode changes: oxidative dehydrogenation becomes nonoxidative.

Additional complication of the catalyst composition (the addition of bismuth and barium to the supported component) results in a further increase in the amount of active oxygen and an increase in the strength of its

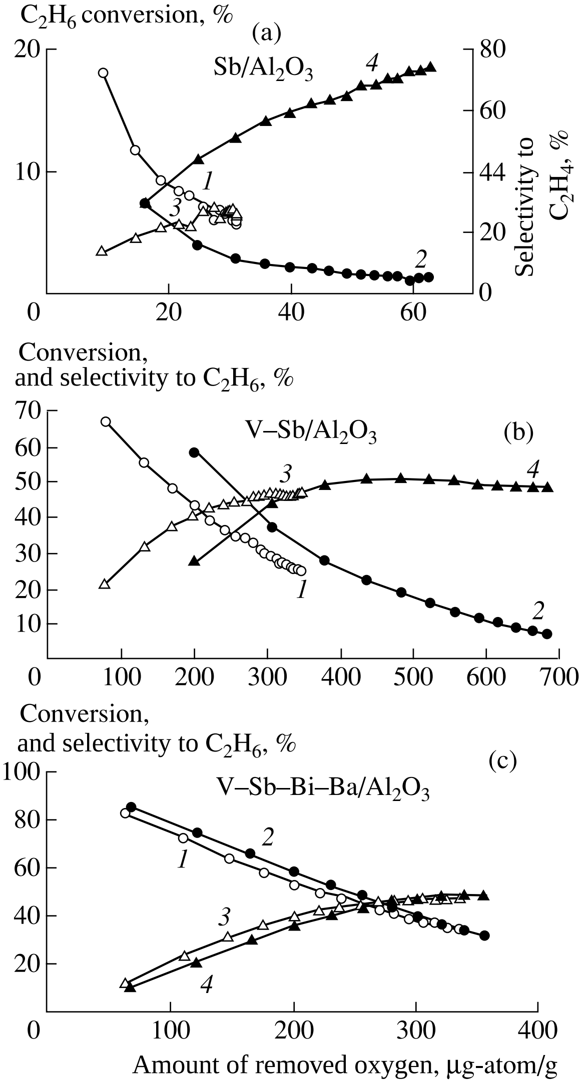

Fig. 8. Dependence of (*1*, *2*) ethane conversion and (*3*, *4*) selectivity to ethylene on the amount of oxygen removed in the reaction of (a) Sb/Al_2O_3, (b) $V–Sb/Al_2O_3$, and (c) $V–Sb–Bi–Ba/Al_2O_3$ with pulses (*1*, *3*) ethane + air + helium and (2, *4*) ethane + helium.

binding to the lattice. However, the heats measured for all the three vanadium-containing systems correspond to the energetics of transitions between V^{3+} and V^{5+}. That is, we may consider that these ions determine the redox properties of systems under study.

Results shown in Fig. 6 point to a continuous increase in the binding strength of oxygen to be removed with oxide and to a complex change in ethane oxidation selectivity, which has a flat maximum at 300–400 μg-atom O per gram of the sample. The high fraction of carbon oxides at low extents of reduction can be explained by the presence of active oxygen with low binding energies and a relatively large amount of reactive oxygen in the oxide at this stage. On the contrary, the observed decrease in the selectivity to ethylene with an increase in the extent of sample reduction from 400 to 500 μg-atom O/g takes place when the binding strength of lattice oxygen is higher. This effect is reproducible in the experiments with different ethane concentrations in reactant pulses. In this case, an increase in the extent of hydrocarbon oxidation is probably due to an increase in the lifetime of carbon-containing intermediates on the oxide surface resulting in the higher probability of their further oxidation to form carbon oxides. This, in turn, can result from the formation of low-coordination ions of reduced vanadium on which firmer adsorption of organic molecules is possible. The partial reduction of bismuth oxide to metallic bismuth [15] also can be another reason for this effect.

Comparison of experimental results on the interaction between the oxide system and ethane pulses with and without oxygen supports the idea that vanadium-containing samples conduct the oxidative dehydrogenation of ethane via the redox mechanism. Figure 8 summarizes various dependences of ethane conversion and selectivity to ethylene on the extent of reduction of the $V–Sb/Al_2O_3$ and $V–Sb–Bi–Ba/Al_2O_3$ samples. As noted in the introduction to this paper, the proximity of these values measured in the catalytic and reductive processes points to the occurrence of the catalytic reaction via the reduction–reoxidation Mars–van Krevelen mechanism [7].

At the steady state, a certain extent of catalyst reduction is achieved, which depends on the ethane-to-oxygen ratio in the initial mixture. It is seen from Table 2 that, for the $V–Sb/Al_2O_3$ and $V–Sb–Bi–Ba/Al_2O_3$ samples, the steady-state degree of reduction was ~340 μg-atom O/g. The selectivity of the catalytic process (47.1 and 47.5%, respectively) should be close to the selectivity of the simple sample reduction by oxy-

Table 2. The results of the interaction of samples with 15% ethane + 25% air + helium pulses at 550°C in the "stationary" region

Sample	$X_{C_2H_6}$, %	X_{O_2}, %	C_{CO}, %	C_{CO_2}, %	$C_{C_2H_4}$, %	S_1, %	ΣO, μg-atom/g
$V–Sb–Bi–Ba/Al_2O_3$	34.5	95.2	2.67	2.27	2.24	47.5	335
$V–Sb/Al_2O_3$	24.9	95.4	2.69	1.08	1.68	47.1	347
Sb/Al_2O_3	5.8	29.5	0.53	0.55	0.19	26.5	31

Note: $X_{C_2H_6}$ and X_{O_2} are the conversions of ethane and oxygen, respectively; C_i is the concentration of the reaction products; S_1 is the selectivity to ethylene; ΣO is the overall amount of oxygen removed from the catalyst from the first to the last pulse.

gen-free ethane (~48%) when the same extent of reduction is achieved. This is observed in Figs. 5, 6a, and 8.

Earlier [4], we showed that the optimal efficiency of supported vanadium catalysts is observed at an paraffin : oxygen ratio of 2–3 : 1 and that oxide additives improve the catalytic properties of samples. Results obtained in this work help to understand better the reasons for these dependences. Since we found that the reaction occurs via the reduction–reoxidation mechanism, the highest ethylene yield should be observed at a steady-state extent of catalyst reduction (~300 μg-atom O/g). Because the rate of oxidation by oxygen for our samples is much higher than the rate of reduction by ethane, it is necessary to use the reaction mixture enriched in the reducing agent (paraffin) to achieve this high steady-state degree of reduction.

Furthermore, it is seen from Fig. 7 that, at extents of reduction of ~300–400 μg-atom O/g, the V–Sb–Bi–Ba/Al_2O_3 sample is characterized by a higher rate of reduction by ethane (higher ethane conversion in the C_2H_6–He pulse) than the V–Sb/Al_2O_3 sample. Correspondingly, in the case of ethane–air–helium pulses under pseudostationary conditions, a high conversion of ethane and a high yield of ethylene are observed. Thus, additional modification of the catalyst in this case stipulated an increase in the rate of sample reduction by the paraffin.

A different pattern is observed for the Sb/Al_2O_3 system. Compared to vanadium-containing samples, Sb/Al_2O_3 is reduced less readily and oxidized much more slowly. According to Table 2, at the steady state, the catalyst loses 31 μg-atom O/g. At the same time, the steady-state selectivity to ethylene (26.5%) is lower than the selectivity in oxygen-free pulses (50–60%) at a close degree of reduction and is not higher than the selectivity for the reduction of the completely oxidized sample (Fig. 8). It is likely that, during the interaction of Sb/Al_2O_3 with the ethane–air mixture, only a limited fraction of the products are formed due to active oxygen species that we observed in the processes of Sb/Al_2O_3 reduction. However, because these species are present in a smaller amount (compared to other samples) and because its recovery is slow at 550°C, this process does not result in a high conversion of starting reactants. All data suggest that another short-lived form of oxygen exists on Sb/Al_2O_3 in the presence of gas-phase oxygen under stationary conditions. This form of oxygen reacts with ethane to produce mostly carbon oxides.

CONCLUSION

Thus, we showed that all studied samples contain active oxygen capable of reacting with ethane. The vanadium-containing samples contain the largest amount of reactive oxygen. The addition of the second supported component (antimony oxide) leads to a substantial increase in the amount and reactivity of catalyst oxygen, to the formation of the additional form of active oxygen, and to a substantial decrease in the rate of coking during interaction with ethane.

ACKNOWLEDGMENTS

This work was supported by the grant ERBIC-15-CT-0725 from INCO-Copernicus Program of the European Community.

REFERENCES

1. Kung, H.H., *Adv. Catal.*, 1992, vol. 40, p. 1.
2. Alvonetti, S., Cavani, F., and Trifiro, F., *Catal. Rev. – Sci. Eng.*, 1996, vol. 38, p. 413.
3. Mamedov, E.A. and Cortes Corberan, V., *Appl. Catal., A*, 1995, vol. 127, no. 1, p. 1.
4. Vislovskiy, V.P., Bychkov, V.Yu., Sinev, M.Yu., *et al.*, *Proc. ISO'99, Rimini*, 1999, p. 53.
5. Bañares, M.A., *Catal. Today*, 1999, vol. 51, no. 2, p. 319.
6. Centi, G., *Appl. Catal., A*, 1996, vol. 147, p. 267.
7. Mars, P. and van Krevelen, D.W., *Chem. Eng. Sci.*, 1954, vol. 3, p. 41.
8. Sinev, M.Yu., Korchak, V.N., and Krylov, O.V., *Proc. 6th Int. Symp. on Heterogeneous Catalysis*, Sofia, 1987, part. 1, p. 450.
9. Sinev, M.Yu. and Bychkov, V.Yu., *Kinet. Katal.*, 1999, vol. 40, no. 6, p. 906.
10. Bychkov, V.Yu., Sinev, M.Yu., Korchak, V.N., *et al.*, *Kinet. Katal.*, 1989, vol. 30, no. 5, p. 1137.
11. *Termicheskie konstanty veshchestv* (Thermal Properties of Substances), Moscow: VINITI, 1965–1974, nos. I–VII.
12. Volkov, V.L., *Fazy vnedreniya na osnove oksidov vanadiya* (Interstitial Phases Based on Vanadium Oxides), Sverdlovsk: Ural. Nauchn. Tsentr, Akad. Nauk SSSR, 1987, p. 5.
13. Andersen, P.J. and Kung, H.H., *J. Phys. Chem.*, 1991, vol. 96, no. 7, p. 3114.
14. Bars, J.Le., Auroux, A., Forrissier, M., and Vedrine, J.C., *J. Catal.*, 1996, vol. 162, no. 2, p. 250.
15. DiCosimo, R., Burrington, J., and Grasselli, R.K., *J. Catal.*, 1986, vol. 102, no. 1, p. 234.